

RELATIVISTIC ENERGY DENSITY FUNCTIONALS: BEYOND THE MEAN-FIELD APPROXIMATION*

D. VRETENAR, T. NIKŠIĆ

Physics Department, Faculty of Science, University of Zagreb, Croatia

(Received December 22, 2010)

Relativistic energy density functionals (EDF) provide a complete and accurate description of nuclear ground states and collective excitations. Employing semi-empirical functionals adjusted to the nuclear matter equation of state and to bulk properties of finite nuclei, this framework has been applied to studies of arbitrarily heavy nuclei, exotic nuclei far from stability, and even systems at the nucleon drip-lines. EDF-based structure models have also been developed that go beyond the static mean-field approximation, and include correlations related to the restoration of broken symmetries and to fluctuations of collective variables.

DOI:10.5506/APhysPolB.42.405

PACS numbers: 21.60.Jz, 21.60.Ev, 21.10.Re

1. Introduction

Nuclear energy density functionals (NEDF) provide a microscopic, globally accurate, and yet economic description of ground-state properties and collective excitations over the whole nuclide chart. The basic implementation is in terms of self-consistent mean-field (SCMF) models, in which an EDF is constructed as a functional of one-body nucleon density matrices that correspond to a single product state — Slater determinant of single-particle or single-quasiparticle states. Nuclear SCMF models effectively map the many-body problem onto a one-body problem, and the exact EDF is approximated by a functional of powers and gradients of ground-state nucleon densities and currents, representing distributions of matter, spins, momentum and kinetic energy. In principle, the nuclear EDF can incorporate short-range correlations related to the repulsive core of the inter-nucleon interaction, and long-range correlations mediated by nuclear resonance modes. When considering applications, however, an important challenge for the framework of

* Presented at the Zakopane Conference on Nuclear Physics “Extremes of the Nuclear Landscape”, August 30–September 5, 2010, Zakopane, Poland.

EDF is the systematic treatment of collective correlations related to restoration of broken symmetries and fluctuations of collective coordinates. A static nuclear EDF is characterized by symmetry breaking — translational, rotational, particle number, and can only provide an approximate description of bulk ground-state properties. To calculate excitation spectra and electromagnetic transition rates in individual nuclei, it is necessary to extend the SCMF scheme to include correlations that arise from symmetry restoration and fluctuations around the mean-field minimum. Collective correlations are sensitive to shell effects, display pronounced variations with particle number and, therefore, cannot be incorporated in a universal density functional.

An important class of nuclear structure models belongs to the framework of relativistic energy density functionals (REDF). In particular, models based on the relativistic mean-field (RMF) approximation have been employed very successfully in analyses of ground-state properties, not only in nuclei along the valley of β -stability, but also in exotic nuclei with extreme isospin values and close to the particle drip lines. Applications have reached a level of accuracy comparable to the non-relativistic Hartree–Fock–Bogoliubov approach based on Skyrme functionals or Gogny effective interactions [1, 2, 3, 4, 5]. The nucleon spin degree of freedom is included in a natural way in the framework of REDFs, and the resulting nuclear spin–orbit potential emerges automatically with the empirical strength. The consistent treatment of large isoscalar, Lorentz scalar and vector self-energies, provides a unique parametrization of time-odd components of the nuclear mean-field, *i.e.* nucleon currents, that is absent in the non-relativistic representation of the energy density functional. The empirical pseudospin symmetry in nuclear spectroscopy finds a natural explanation in terms of relativistic mean fields, and a covariant framework provides a consistent treatment of symmetric and asymmetric nuclear matter. In this work, we review recent advances in the framework of relativistic EDFs and, in particular, the latest extensions that include the treatment of collective correlations.

2. The relativistic energy density functional DD-PC1

The basic building blocks of a relativistic nuclear energy density functional are the densities and currents bilinear in the Dirac spinor field ψ of the nucleon

$$\bar{\psi}\mathcal{O}_\tau\Gamma\psi, \quad \mathcal{O}_\tau \in \{1, \tau_i\}, \quad \Gamma \in \{1, \gamma_\mu, \gamma_5, \gamma_5\gamma_\mu, \sigma_{\mu\nu}\}. \quad (1)$$

τ_i are the isospin Pauli matrices and Γ generically denotes the Dirac matrices. The nuclear ground-state density and energy are determined by the self-consistent solution of relativistic linear single-nucleon equations. To derive those equations it is useful to construct an interaction Lagrangian

with four-fermion (contact) interaction terms in the various isospace–space channels: isoscalar–scalar $(\bar{\psi}\psi)^2$, isoscalar–vector $(\bar{\psi}\gamma_\mu\psi)(\bar{\psi}\gamma^\mu\psi)$, isovector–scalar $(\bar{\psi}\vec{\tau}\psi) \cdot (\bar{\psi}\vec{\tau}\psi)$, isovector–vector $(\bar{\psi}\vec{\tau}\gamma_\mu\psi) \cdot (\bar{\psi}\vec{\tau}\gamma^\mu\psi)$. A general Lagrangian can be written as a power series in the currents $\bar{\psi}\mathcal{O}_\tau\Gamma\psi$ and their derivatives, with higher-order terms representing in-medium many-body correlations. In Ref. [6] a Lagrangian was considered that includes second-order interaction terms, with many-body correlations encoded in density-dependent strength functions

$$\begin{aligned} \mathcal{L} = & \bar{\psi}(i\gamma \cdot \partial - m)\psi \\ & - \frac{1}{2}\alpha_S(\hat{\rho})(\bar{\psi}\psi)(\bar{\psi}\psi) - \frac{1}{2}\alpha_V(\hat{\rho})(\bar{\psi}\gamma^\mu\psi)(\bar{\psi}\gamma_\mu\psi) \\ & - \frac{1}{2}\alpha_{\text{TV}}(\hat{\rho})(\bar{\psi}\vec{\tau}\gamma^\mu\psi)(\bar{\psi}\vec{\tau}\gamma_\mu\psi) \\ & - \frac{1}{2}\delta_S(\partial_\nu\bar{\psi}\psi)(\partial^\nu\bar{\psi}\psi) - e\bar{\psi}\gamma \cdot A\frac{(1-\tau_3)}{2}\psi. \end{aligned} \quad (2)$$

In addition to the free-nucleon Lagrangian and the interaction terms, when applied to nuclei, the model must include the coupling of protons to the electromagnetic field. The derivative term in Eq. (2) accounts for leading effects of finite-range interactions that are crucial for a quantitative description of nuclear density distributions, *e.g.* nuclear radii. Similar interactions can be included in each space–isospace channel. In practice, however, data on charge radii can only constrain a single derivative term. The Lagrangian (2) includes an isovector–vector but not an isovector–scalar term. Although the total isovector strength is relatively well-defined, the distribution between the scalar and vector channels is not determined by ground-state data.

The single-nucleon Dirac equation is obtained from the variation of the Lagrangian with respect to $\bar{\psi}$

$$[\gamma_\mu(i\partial^\mu - \Sigma^\mu - \Sigma_{\text{R}}^\mu) - (m + \Sigma_{\text{S}})]\psi = 0 \quad (3)$$

with the nucleon self-energies defined by the following relations:

$$\Sigma^\mu = \alpha_V(\rho_v)j^\mu + e\frac{(1-\tau_3)}{2}A^\mu, \quad (4)$$

$$\Sigma_{\text{R}}^\mu = \frac{1}{2}\frac{j^\mu}{\rho_v} \left\{ \frac{\partial\alpha_S}{\partial\rho}\rho_s^2 + \frac{\partial\alpha_V}{\partial\rho}j_\mu j^\mu + \frac{\partial\alpha_{\text{TV}}}{\partial\rho}\vec{j}_\mu\vec{j}^\mu \right\}, \quad (5)$$

$$\Sigma_{\text{S}} = \alpha_S(\rho_v)\rho_s - \delta_S\Box\rho_s, \quad (6)$$

$$\Sigma_{\text{TV}}^\mu = \alpha_{\text{TV}}(\rho_v)\vec{j}^\mu. \quad (7)$$

In addition to the contributions of the isoscalar–vector four-fermion interaction and the electromagnetic interaction, the isoscalar–vector self-energy Σ^μ includes the “rearrangement” terms Σ_{R}^μ . The latter arise from the variation of the vertex functionals α_S , α_V , and α_{TV} with respect to the nucleon

fields in the vector density operator $\hat{\rho}_v$. The inclusion of the rearrangement self-energy is essential for energy-momentum conservation and the thermodynamical consistency of the model. Σ_S and Σ_{TV}^μ denote the isoscalar–scalar and isovector–vector self-energies, respectively.

In the relativistic density functional framework the nuclear ground state $|\phi_0\rangle$ is represented by the self-consistent mean-field solution of the system of equations (3)–(7). The isoscalar and isovector four-currents and scalar density read

$$j_\mu = \langle \bar{\psi} \gamma_\mu \psi \rangle = \sum_{k=1}^N v_k^2 \bar{\psi}_k \gamma_\mu \psi_k, \quad (8)$$

$$\vec{j}_\mu = \langle \bar{\psi} \gamma_\mu \vec{\tau} \psi \rangle = \sum_{k=1}^N v_k^2 \bar{\psi}_k \gamma_\mu \vec{\tau} \psi_k, \quad (9)$$

$$\rho_S = \langle \bar{\psi} \psi \rangle = \sum_{k=1}^N v_k^2 \bar{\psi}_k \psi_k. \quad (10)$$

ψ_k are Dirac spinors, and the sum runs over occupied positive-energy single-nucleon orbitals, including the corresponding occupation factors v_k^2 . The single-nucleon Dirac equations are solved self-consistently in the “no-sea” approximation that omits the explicit contribution of negative-energy solutions of the relativistic equations to the densities and currents.

Most NEDFs have been determined by empirical parameters adjusted to ground-state data (masses, charge radii) of a relatively small number of spherical closed-shell nuclei. In Ref. [6] a set of 10 constants that control the strength and density dependence of the interaction terms of the Lagrangian Eq. (2), was fine-tuned in a multistep parameter fit exclusively to the experimental masses of 64 axially deformed nuclei in the regions $A \approx 150$ –180 and $A \approx 230$ –250. The resulting functional DD-PC1 has been further tested in calculations of binding energies, charge radii, deformation parameters, neutron skin thickness, and excitation energies of giant monopole and dipole resonances. The corresponding nuclear matter equation of state is characterized by the following properties at the saturation point: nucleon density $\rho_{\text{sat}} = 0.152 \text{ fm}^{-3}$, volume energy $a_v = -16.06 \text{ MeV}$, surface energy $a_s = 17.498 \text{ MeV}$, symmetry energy $a_4 = 33 \text{ MeV}$, and the nuclear matter compression modulus $K_{\text{nm}} = 230 \text{ MeV}$.

For a quantitative description of open-shell nuclei it is necessary to consider also pairing correlations. The relativistic Hartee–Bogoliubov (RHB) framework [3] provides a unified description of particle–hole (ph) and particle–particle (pp) correlations on a mean-field level by combining two average potentials: the self-consistent mean field that encloses all the long range ph

correlations, and a pairing field $\hat{\Delta}$ which sums up the pp -correlations. In this work we present results that are based on RHB calculations with the ph effective interaction derived from the DD-PC1 functional, and a pairing force separable in momentum space: $\langle k | V^{1S_0} | k' \rangle = -Gp(k)p(k')$ is used in the pp channel. By assuming a simple Gaussian ansatz $p(k) = e^{-a^2k^2}$, the two parameters G and a have been adjusted to reproduce the density dependence of the gap at the Fermi surface in nuclear matter, calculated with a Gogny force. For the D1S parameterization [8] of the Gogny force: $G = -728 \text{ MeV fm}^3$ and $a = 0.644 \text{ fm}$. When transformed from momentum to coordinate space, the force takes the form

$$V(\mathbf{r}_1, \mathbf{r}_2, \mathbf{r}'_1, \mathbf{r}'_2) = G\delta(\mathbf{R} - \mathbf{R}') P(\mathbf{r})P(\mathbf{r}') \frac{1}{2}(1 - P^\sigma), \quad (11)$$

where $\mathbf{R} = \frac{1}{2}(\mathbf{r}_1 + \mathbf{r}_2)$ and $\mathbf{r} = \mathbf{r}_1 - \mathbf{r}_2$ denote the center-of-mass and the relative coordinates, and $P(\mathbf{r})$ is the Fourier transform of $p(k)$

$$P(\mathbf{r}) = \frac{1}{(4\pi a^2)^{3/2}} e^{-\mathbf{r}^2/4a^2}. \quad (12)$$

The pairing force is of finite range and, because of the presence of the factor $\delta(\mathbf{R} - \mathbf{R}')$, it preserves translational invariance. Even though $\delta(\mathbf{R} - \mathbf{R}')$ implies that this force is not completely separable in coordinate space, the corresponding pp matrix elements can be represented as a sum of a finite number of separable terms in the basis of a 3D harmonic oscillator. The force Eq. (11) reproduces pairing properties of spherical and deformed nuclei calculated with the original Gogny force, but with the important advantage that the computational cost is greatly reduced.

3. Beyond the mean-field approximation: shape evolution in neutron-deficient Kr isotopes

A quantitative description of structure phenomena related to shell evolution necessitates the inclusion of many-body correlations beyond the mean-field approximation. In a series of recent papers the framework of relativistic energy density functionals has been expanded to include correlations related to the restoration of broken symmetries and to fluctuations of collective variables. A model has been developed that uses the generator coordinate method (GCM) to perform configuration mixing of angular-momentum [9], and also particle-number projected [10] relativistic wave functions. The geometry is restricted to axially symmetric shapes, and the intrinsic wave functions are generated from the solutions of the relativistic mean-field + Lipkin-Nogami BCS equations, with a constraint on the mass quadrupole

moment. This approach has been further developed in Refs. [11] by implementing a model that includes triaxial angular-momentum projection, although without projection on nucleon number.

In an alternative approach to five-dimensional quadrupole dynamics that restores rotational symmetry and takes into account fluctuations around the triaxial mean-field minimum, a collective Bohr Hamiltonian can be formulated. The corresponding deformation-dependent parameters are determined from self-consistent relativistic mean-field calculations for triaxial shapes [12]. Here, we illustrate this approach with a configuration mixing calculation of Kr isotopes, based on triaxial RHB shapes computed with the DD-PC1 functional.

Neutron-deficient nuclei in the mass region $A \approx 70\text{--}80$ are predicted to display coexisting prolate and oblate shapes, as a result of competing large shell gaps for both prolate and oblate deformations at proton/neutron number 34, 36, and 38. In Fig. 1 we display the 3D RHB binding energy maps of the even- A Kr isotopes: ^{72}Kr , ^{74}Kr , ^{76}Kr and ^{78}Kr , calculated using the DD-PC1 energy density functional plus the pairing interaction Eq. (11). The map of the energy surface as a function of the quadrupole deformation is obtained by imposing constraints on the axial and triaxial quadrupole moments. All four isotopes appear to be rather soft with respect to both β and γ degrees of freedom. The occurrence of nearly degenerate minima raises the question of their stability against dynamical effects of collective correlations.

The entire dynamics of the collective Hamiltonian is governed by the seven functions of the intrinsic deformations β and γ : the collective potential, the three mass parameters: $B_{\beta\beta}$, $B_{\beta\gamma}$, $B_{\gamma\gamma}$, and the three moments of inertia \mathcal{I}_k . These functions are determined by the choice of a particular microscopic nuclear energy density functional or effective interaction. The quasiparticle wave functions and energies, that correspond to constrained self-consistent solutions of the RHB model, provide the microscopic input for the parameters of the collective Hamiltonian

$$\hat{H} = \hat{T}_{\text{vib}} + \hat{T}_{\text{rot}} + V_{\text{coll}}, \quad (13)$$

with the vibrational kinetic energy

$$\begin{aligned} \hat{T}_{\text{vib}} = & -\frac{\hbar^2}{2\sqrt{wr}} \left\{ \frac{1}{\beta^4} \left[\frac{\partial}{\partial\beta} \sqrt{\frac{r}{w}} \beta^4 B_{\gamma\gamma} \frac{\partial}{\partial\beta} - \frac{\partial}{\partial\beta} \sqrt{\frac{r}{w}} \beta^3 B_{\beta\gamma} \frac{\partial}{\partial\gamma} \right] \right. \\ & \left. + \frac{1}{\beta \sin 3\gamma} \left[-\frac{\partial}{\partial\gamma} \sqrt{\frac{r}{w}} \sin 3\gamma B_{\beta\gamma} \frac{\partial}{\partial\beta} + \frac{1}{\beta} \frac{\partial}{\partial\gamma} \sqrt{\frac{r}{w}} \sin 3\gamma B_{\beta\beta} \frac{\partial}{\partial\gamma} \right] \right\}, \quad (14) \end{aligned}$$

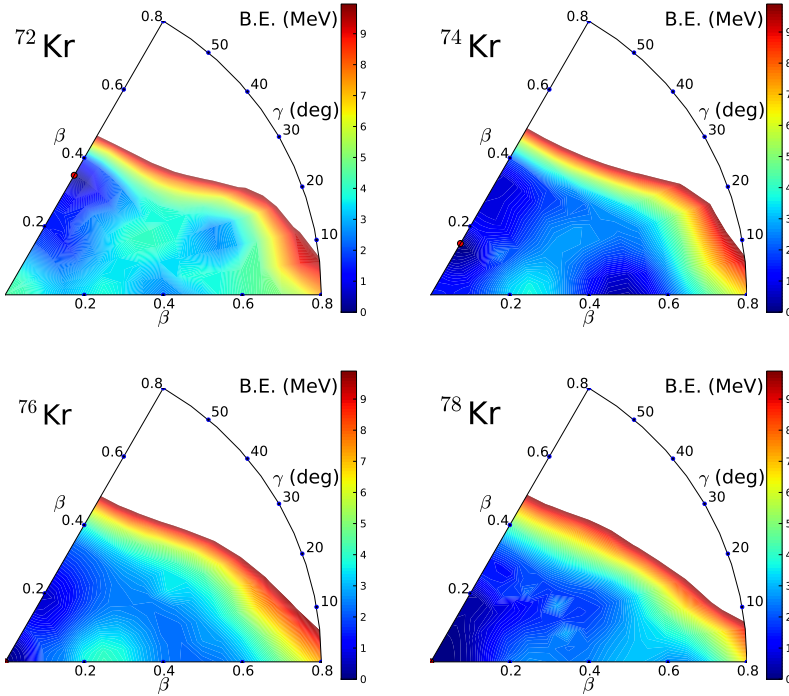


Fig. 1. Self-consistent RHB triaxial quadrupole binding-energy maps of the even–even isotopes $^{72-78}\text{Kr}$ in the β – γ plane ($0 \leq \gamma \leq 60^\circ$). All energies are normalized with respect to the binding energy of the absolute minimum.

and rotational kinetic energy

$$\hat{T}_{\text{rot}} = \frac{1}{2} \sum_{k=1}^3 \frac{\hat{J}_k^2}{\mathcal{I}_k}. \quad (15)$$

V_{coll} is the collective potential. \hat{J}_k denotes the components of the angular momentum in the body-fixed frame of a nucleus, and the mass parameters $B_{\beta\beta}$, $B_{\beta\gamma}$, $B_{\gamma\gamma}$, as well as the moments of inertia \mathcal{I}_k , depend on the quadrupole deformation variables β and γ : $\mathcal{I}_k = 4B_k\beta^2 \sin^2(\gamma - 2k\pi/3)$. Two additional quantities that appear in the expression for the vibrational energy: $r = B_1B_2B_3$, and $w = B_{\beta\beta}B_{\gamma\gamma} - B_{\beta\gamma}^2$, determine the volume element in the collective space. The moments of inertia are computed using the Inglis–Belyaev formula, and the mass parameters associated with the two quadrupole collective coordinates $q_0 = \langle \hat{Q}_{20} \rangle$ and $q_2 = \langle \hat{Q}_{22} \rangle$ are calculated in the cranking approximation. The potential V_{coll} in the collective Hamiltonian Eq. (13) is obtained by subtracting the zero-point energy corrections

from the total energy that corresponds to the solution of constrained RHB equations, at each point on the triaxial deformation plane. The Hamiltonian Eq. (13) describes quadrupole vibrations, rotations, and the coupling of these collective modes. The corresponding eigenvalue problem is solved using an expansion of eigenfunctions in terms of a complete set of basis functions that depend on the deformation variables β and γ , and the Euler angles ϕ , θ and ψ [12].

In Fig. 2 we display the resulting spectrum of collective states of ^{74}Kr , with the parameters of the collective Hamiltonian determined by the constrained self-consistent solutions of the RHB equations (*cf.* Fig. 1). The calculated excitation energies and intraband and interband $B(E2)$ values are shown in comparison with available data [13]. The theoretical spectrum shows a very good agreement with experiment, not only for the ground-state band but also for the structures observed above the yrast. It should be emphasized that the calculation does not contain additional parameters, that is, the solutions are completely determined by the DD-PC1 energy density functional plus the pairing interaction Eq. (11). Physical observables, such as transition probabilities and spectroscopic quadrupole moments, are calculated in the full configuration space using the bare value of the proton charge.

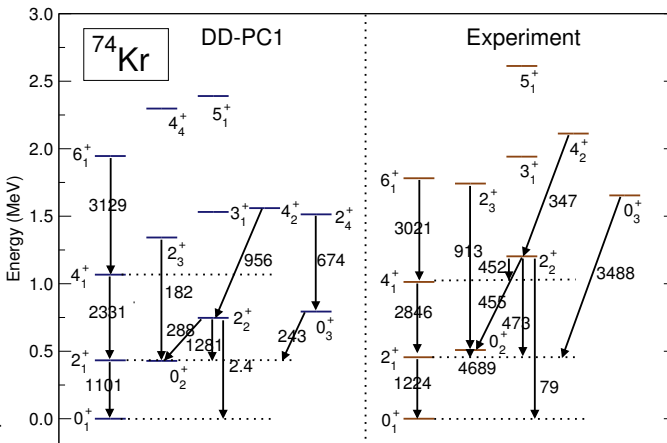


Fig. 2. The low energy spectrum of ^{74}Kr calculated with the DD-PC1 relativistic density functional (left) compared with data (right) for the excitation energies and intraband and interband $B(E2)$ values (in $e^2 \text{ fm}^4$).

A detailed comparison of spectroscopic data with the results of configuration mixing calculations based on the triaxial Hartree–Fock–Bogoliubov model (Gogny D1S effective interaction), and with axial GCM calculations (Skyrme SLy6 force), was reported in Ref. [13]. It was concluded that the

structure of low-lying states in the light krypton isotopes is dominated by the coexistence of prolate and oblate configurations. The ground-state bands of ^{74}Kr and ^{76}Kr , in particular, appear to be based on prolate-deformed minima. For the DD-PC1 theoretical spectrum of ^{74}Kr shown in Fig. 2, the probability densities in the β - γ plane for the yrast states 0_1^+ , 2_1^+ , and 4_1^+ , and the state 0_2^+ , are plotted in Fig. 3. It is interesting to note that the two lowest 0^+ states exhibit a pronounced mixing of oblate and prolate configurations. This mixing can be attributed to the softness of the potential with respect to γ deformation. Even though the ground state is not prolate, the collective functions of the other yrast states are concentrated close to the prolate axis, and the prolate character of these states is also reflected in the calculated spectroscopic moments, which are in agreement with the empirical values [13]. Another distinct feature of the experimental spectrum are the large $B(E2)$ values for the transitions: $0_2^+ \rightarrow 2_1^+$ and $0_3^+ \rightarrow 2_1^+$, which confirm the strong mixing of prolate and oblate structures. In the present calculation the corresponding theoretical $B(E2)$ values are not that large,

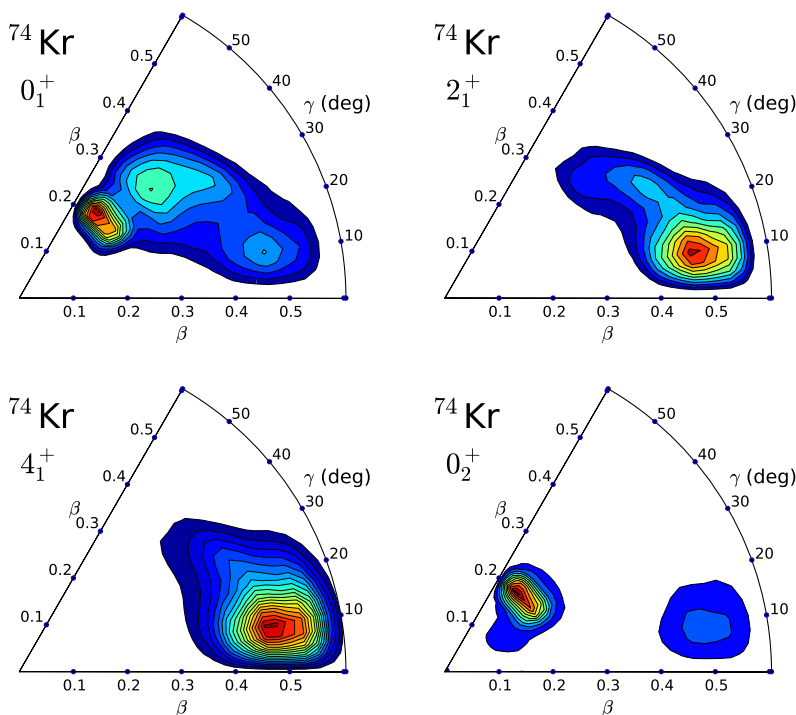


Fig. 3. Probability densities in the β - γ plane for the states 0_1^+ , 2_1^+ , 4_1^+ and 0_2^+ of ^{74}Kr .

for instance $B(E2; 0_2^+ \rightarrow 2_1^+) = 2344 e^2 \text{ fm}^4$ but, nevertheless, the model reproduces the complex structure observed above the yrast in the transitional and γ -soft nucleus ^{74}Kr .

In conclusion, the framework of relativistic energy density functionals provides a global microscopic description of stable nuclei and isotopes far from stability. When extended to take into account collective correlations, this approach can be employed in studies of structure phenomena related to shell evolution, including detailed predictions of excitation spectra and electromagnetic transition rates.

REFERENCES

- [1] G.A. Lalazissis, P. Ring, D. Vretenar (Eds.), *Extended Density Functionals in Nuclear Structure Physics, Lect. Notes Phys.* **641**, Springer, Heidelberg 2004.
- [2] M. Bender, P.-H. Heenen, P.-G. Reinhard, *Rev. Mod. Phys.* **75**, 121 (2003).
- [3] D. Vretenar, A.V. Afanasjev, G.A. Lalazissis, P. Ring, *Phys. Rep.* **409**, 101 (2005).
- [4] J. Meng *et al.*, *Prog. Part. Nucl. Phys.* **57**, 470 (2006).
- [5] N. Paar, D. Vretenar, E. Khan, G. Colò, *Rep. Prog. Phys.* **70**, 691 (2007).
- [6] T. Nikšić, D. Vretenar, P. Ring, *Phys. Rev.* **C78**, 034318 (2008).
- [7] Yuan Tian, Zhong-yu Ma, P. Ring, *Phys. Lett.* **B676**, 44 (2009).
- [8] J.F. Berger, M. Girod, D. Gogny, *Comput. Phys. Commun.* **63**, 365 (1991).
- [9] T. Nikšić, D. Vretenar, P. Ring, *Phys. Rev.* **C73**, 034308 (2006).
- [10] T. Nikšić, D. Vretenar, P. Ring, *Phys. Rev.* **C74**, 064309 (2006).
- [11] J.M. Yao, J. Meng, P. Ring, D. Vretenar, *Phys. Rev.* **C81**, 044311 (2010).
- [12] T. Nikšić *et al.*, *Phys. Rev.* **C79**, 034303 (2009).
- [13] E. Clément *et al.*, *Phys. Rev.* **C75**, 054313 (2007).